Electronic Supplementary Material (ESI) for RSC Advances.

Selective colorimetric sensing of fluoride in aqueous solution by amino-naphthoquinone and its Co(II), Ni(II), Cu(II) and Zn(II) complexes – Effect of complex formation on sensing behaviour

C. Parthiban[a], Samuele Ciattini[b], Laura Chelazzi[b], and Kuppanagounder P. Elango[a*]

Table of Content

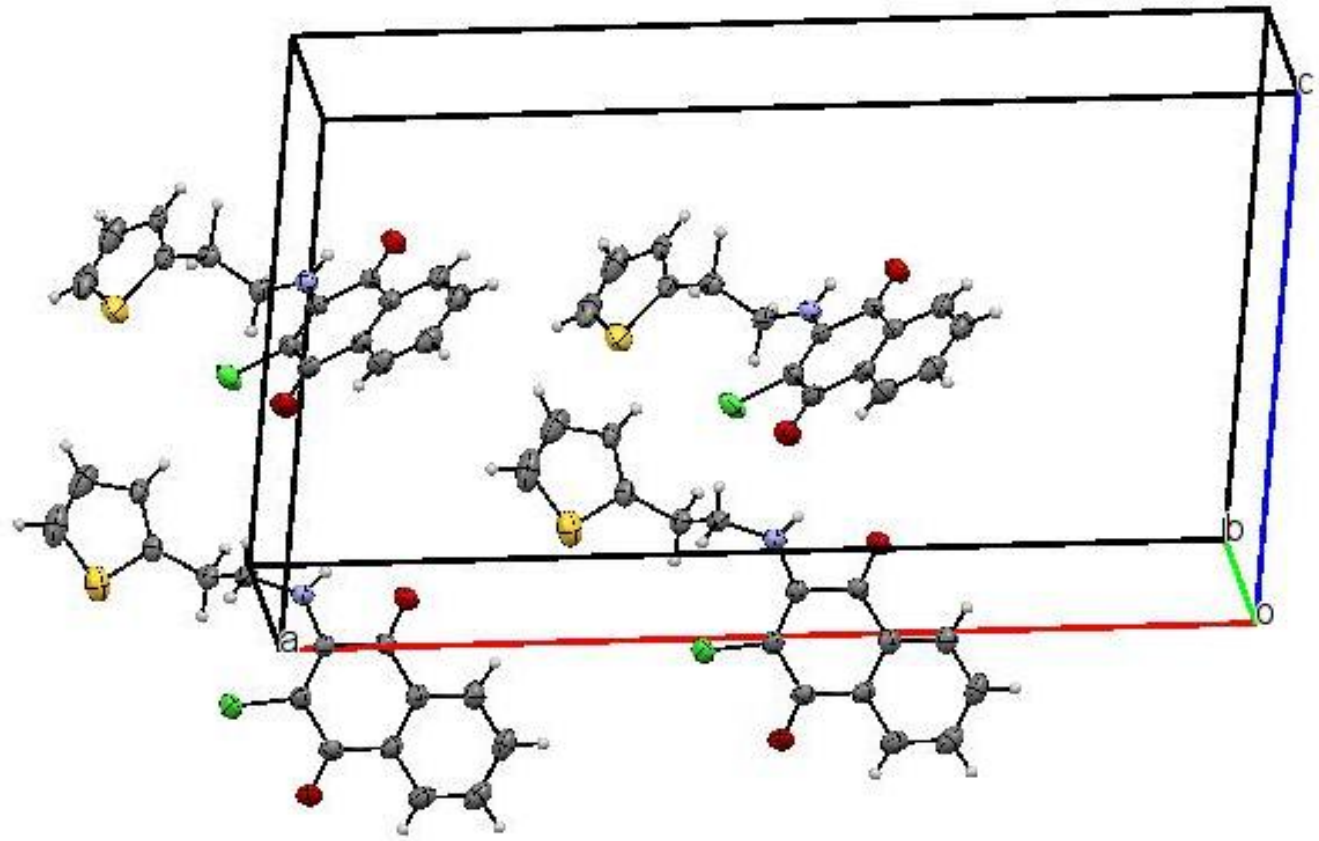

Fig. S1. Crystal packing diagram of **R1**

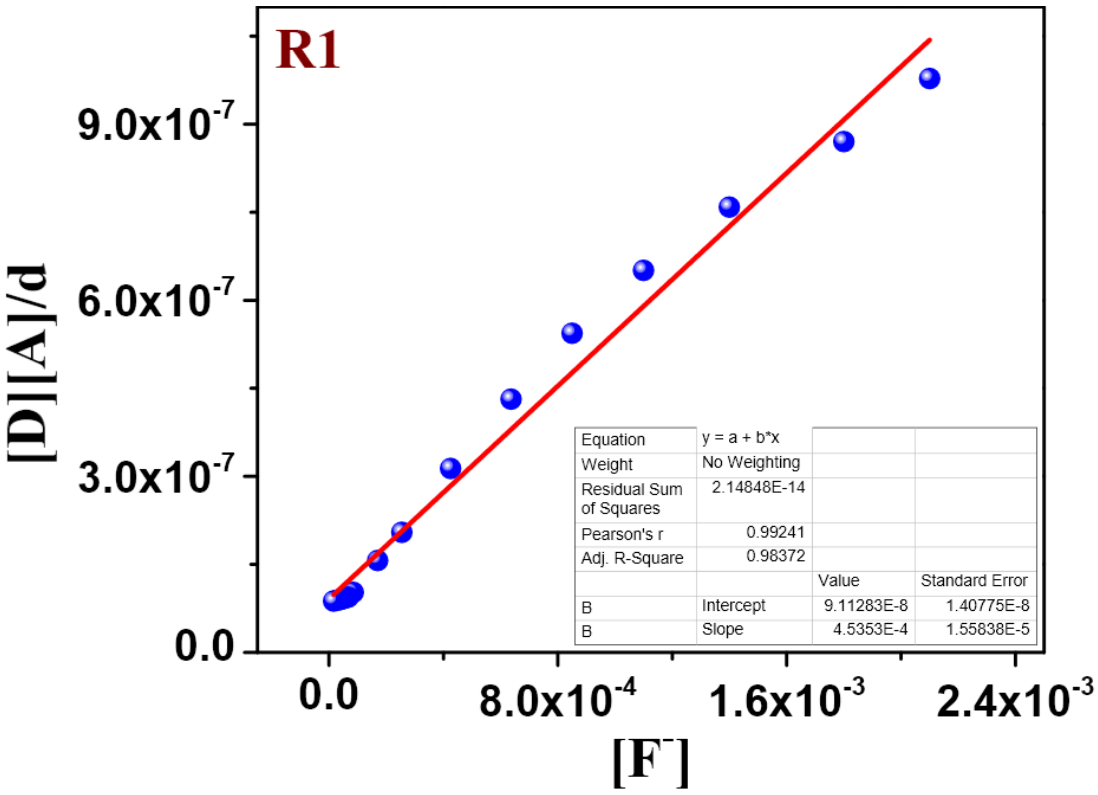
R1
9.0x10-7
6.0x10-7
3.0x10-7
0.0
[D][A]/d
0.0
8.0x10-4
1.6x10-3
2.4x10-3
[F-]
Equation y = a + b*x
Weight No Weighting
Residual Sum of Squares 2.14848E-14
Pearson's r 0.99241
Adj. R-Square 0.98372
Value Standard Error
B Intercept 9.11283E-8 1.40775E-8
B Slope 4.5353E-4 1.55838E-5

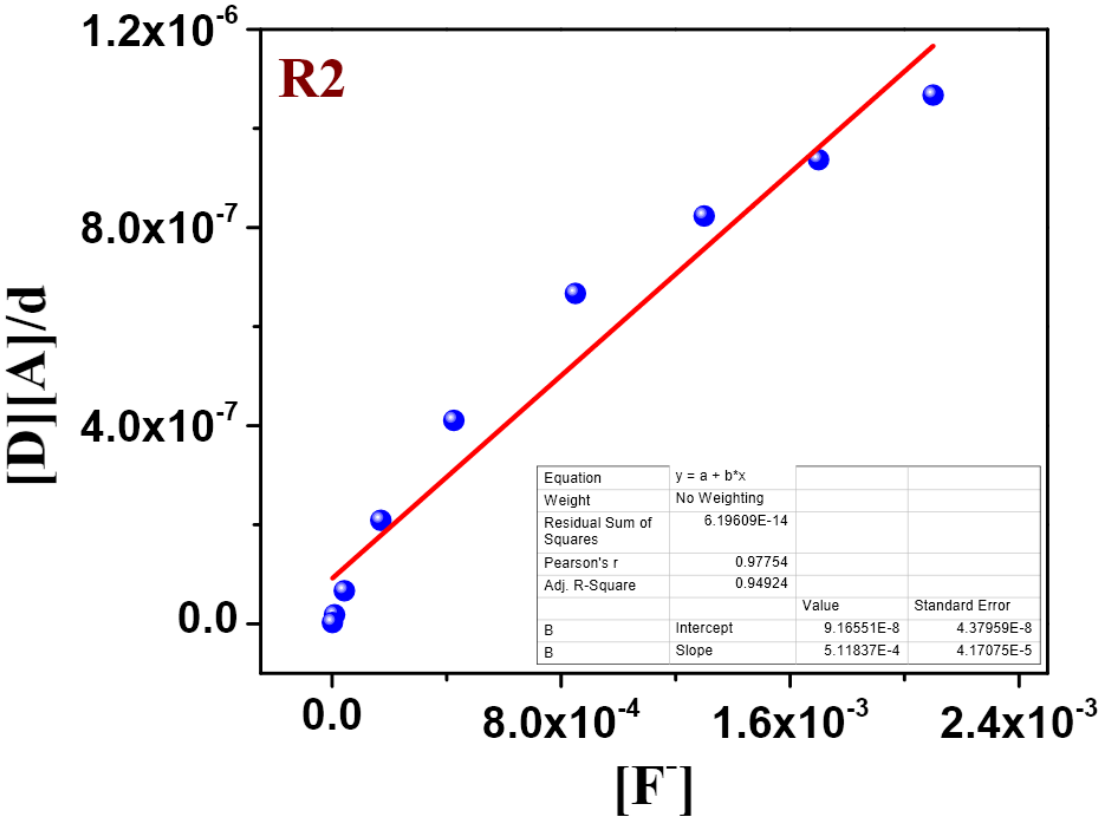
R2
1.2x10-6
8.0x10-7
4.0x10-7
0.0
[D][A]/d
0.0
8.0x10-4
1.6x10-3
2.4x10-3
[F-]
Equation y = a + b*x
Weight No Weighting
Residual Sum of Squares 6.19609E-14
Pearson's r 0.97754
Adj. R-Square 0.94924
Value Standard Error
B Intercept 9.16551E-8 4.37959E-8
B Slope 5.11837E-4 4.17075E-5

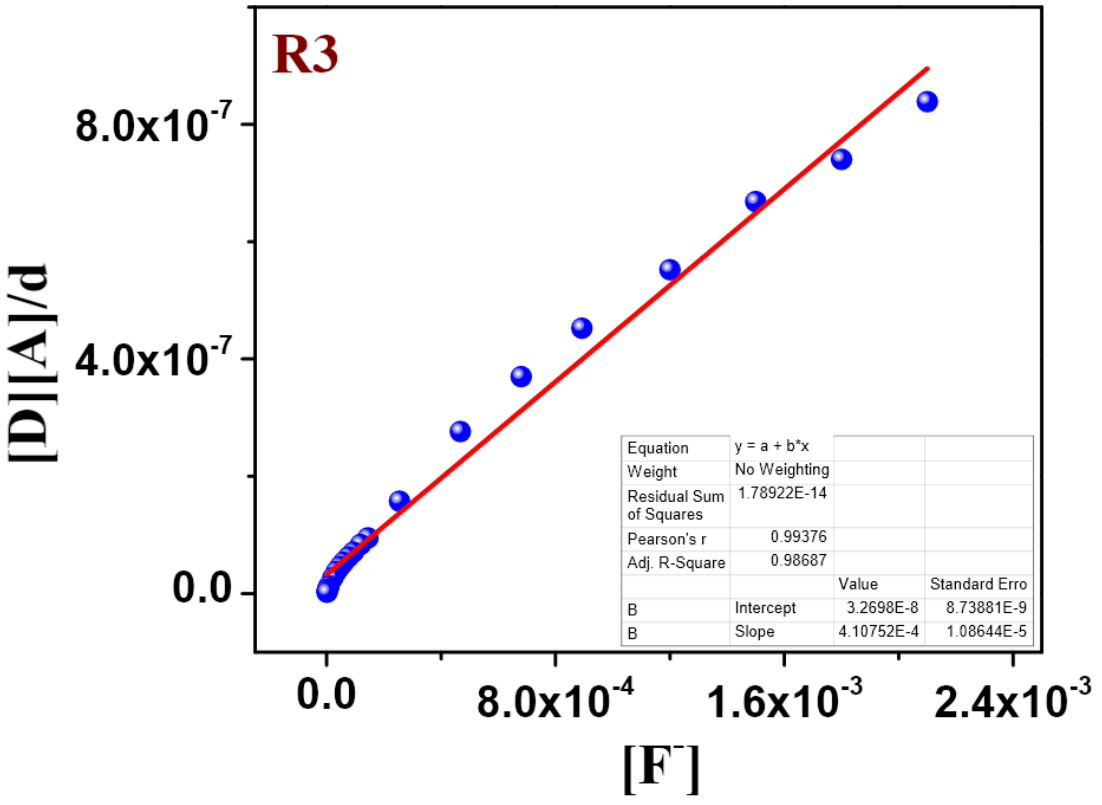
R3
8.0x10-7
4.0x10-7
0.0
[D][A]/d
0.0
8.0x10-4
1.6x10-3
2.4x10-3
[F-]
Equation y = a + b*x
Weight No Weighting
Residual Sum of Squares 1.78922E-14
Pearson's r 0.99376
Adj. R-Square 0.98687
Value Standard Erro
B Intercept 3.2698E-8 8.73881E-9
B Slope 4.10752E-4 1.08644E-5

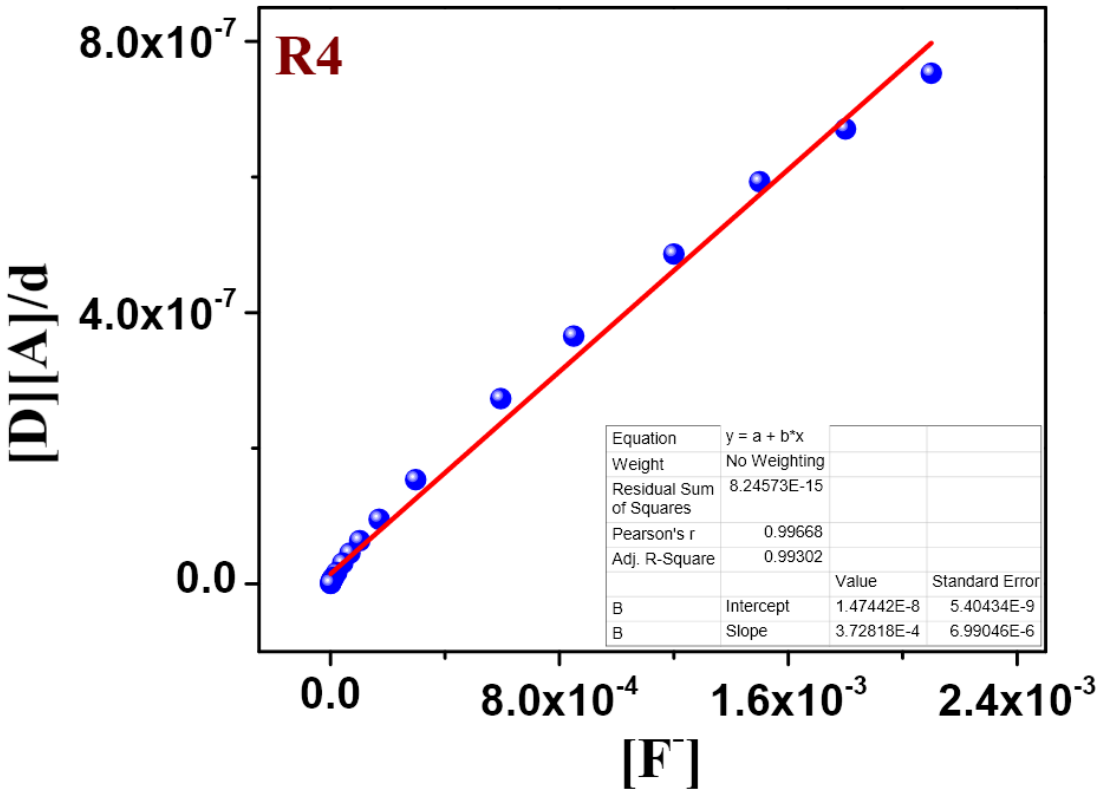
R4
8.0x10-7
4.0x10-7
0.0
[D][A]/d
0.0
8.0x10-4
1.6x10-3
2.4x10-3
[F-]
Equation y = a + b*x
Weight No Weighting
Residual Sum of Squares 8.24573E-15
Pearson's r 0.99668
Adj. R-Square 0.99302
Value Standard Error
B Intercept 1.47442E-8 5.40434E-9
B Slope 3.72818E-4 6.99046E-6

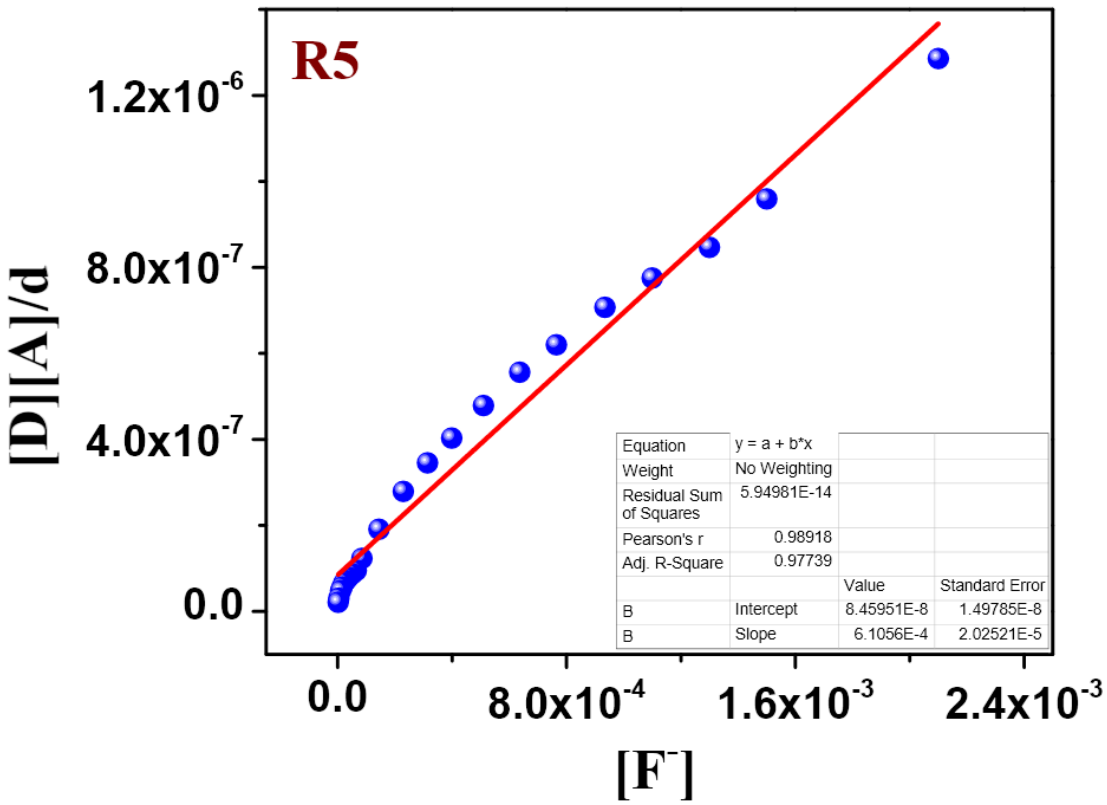
R5
1.2x10-6
8.0x10-7
4.0x10-7
0.0
[D][A]/d
0.0
8.0x10-4
1.6x10-3
2.4x10-3
[F-]
Equation y = a + b*x
Weight No Weighting
Residual Sum of Squares 5.94981E-14
Pearson's r 0.98918
Adj. R-Square 0.97739
Value Standard Error
B Intercept 8.45951E-8 1.49785E-8
B Slope 6.1056E-4 2.02521E-5

Fig. S2. Scott-equation plot of Receptors (**R1-R5**) with F^- ions.

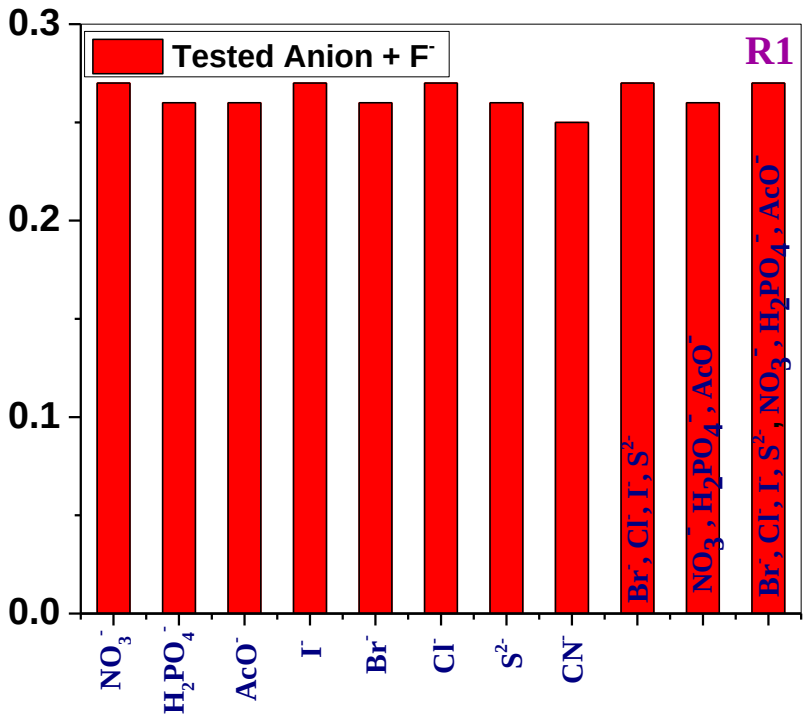

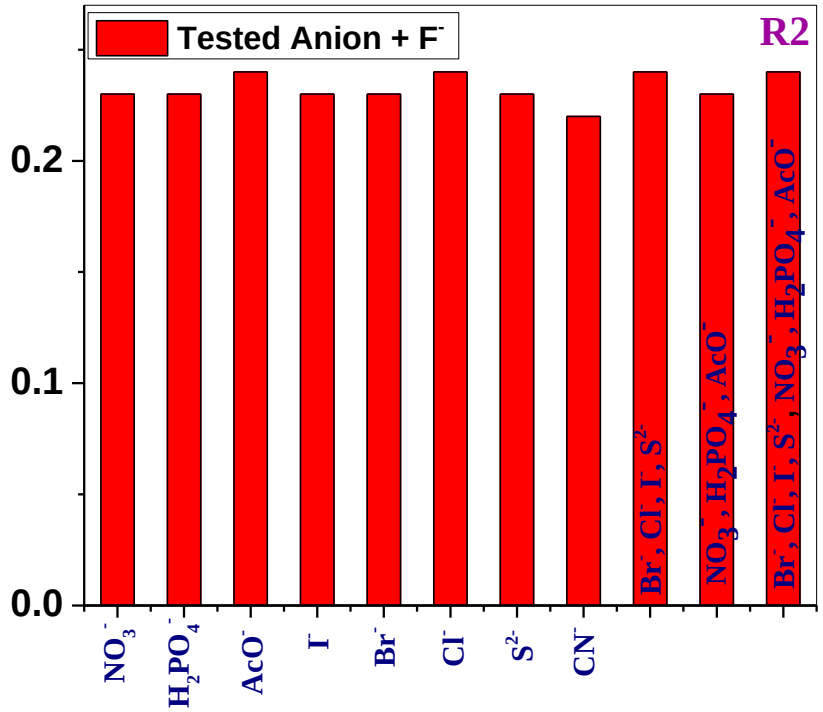
Tested Anion + F-
R2
0.0
0.1
0.2
NO3-
H2PO4-
AcO-
I-
Br-
Cl-
S2-
CN-
Br-, Cl-, I-, S2-
NO3-, H2PO4-, AcO-
Br-, Cl-, I-, S2-, NO3-, H2PO4-, AcO-

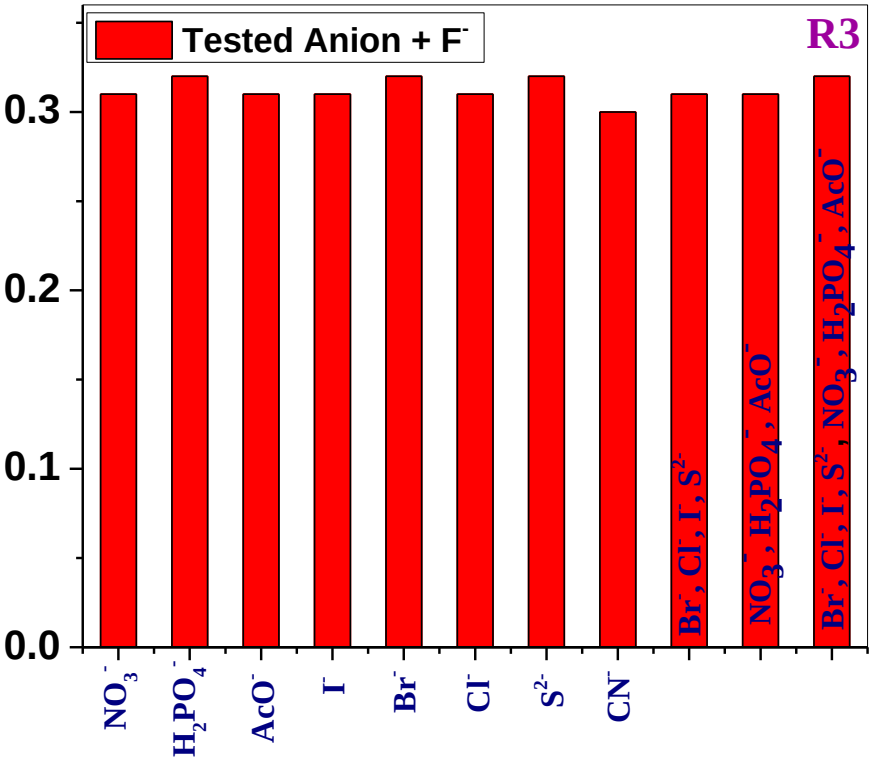
Tested Anion + F-
R3
0.0
0.1
0.2
0.3
NO3-
H2PO4-
AcO-
I-
Br-
Cl-
S2-
CN-
Br-, Cl-, I-, S2-
NO3-, H2PO4-, AcO-
Br-, Cl-, I-, S2-, NO3-, H2PO4-, AcO-

Fig. S3. UV-Vis absorbance intensity response of **R1**-**R5** upon addition of F^- ions.

(**R1** in DMF; **R2**, **R3** and **R5** in 50% aq. DMF and **R4** in 70% aq. DMF solution)

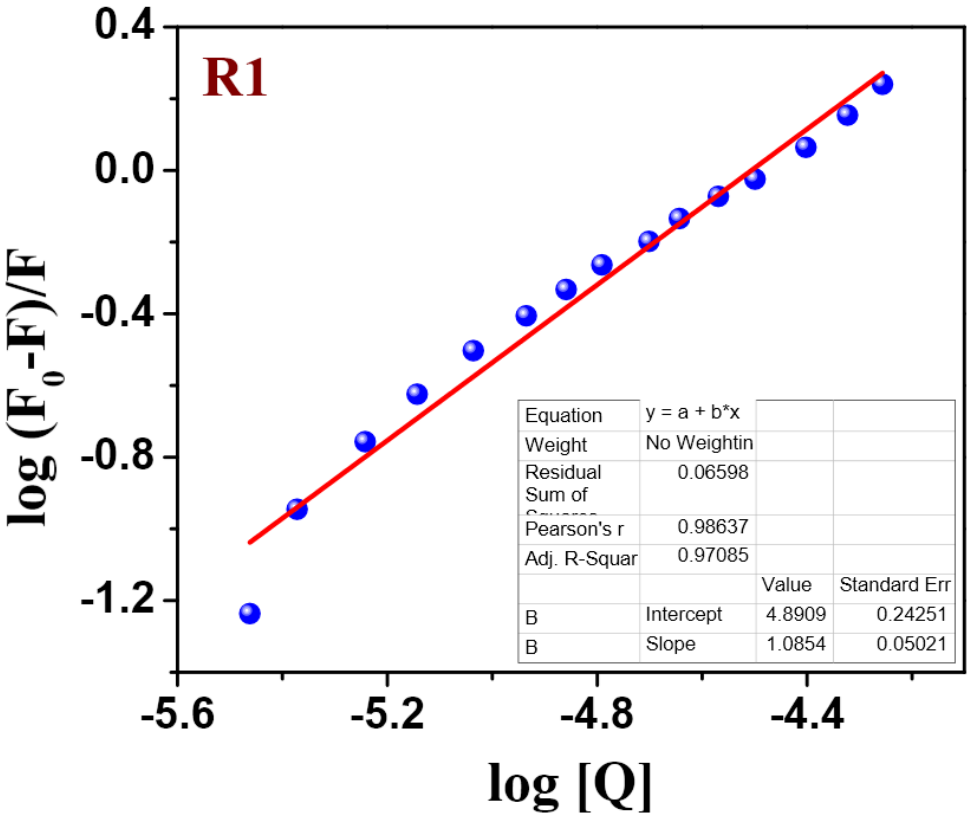

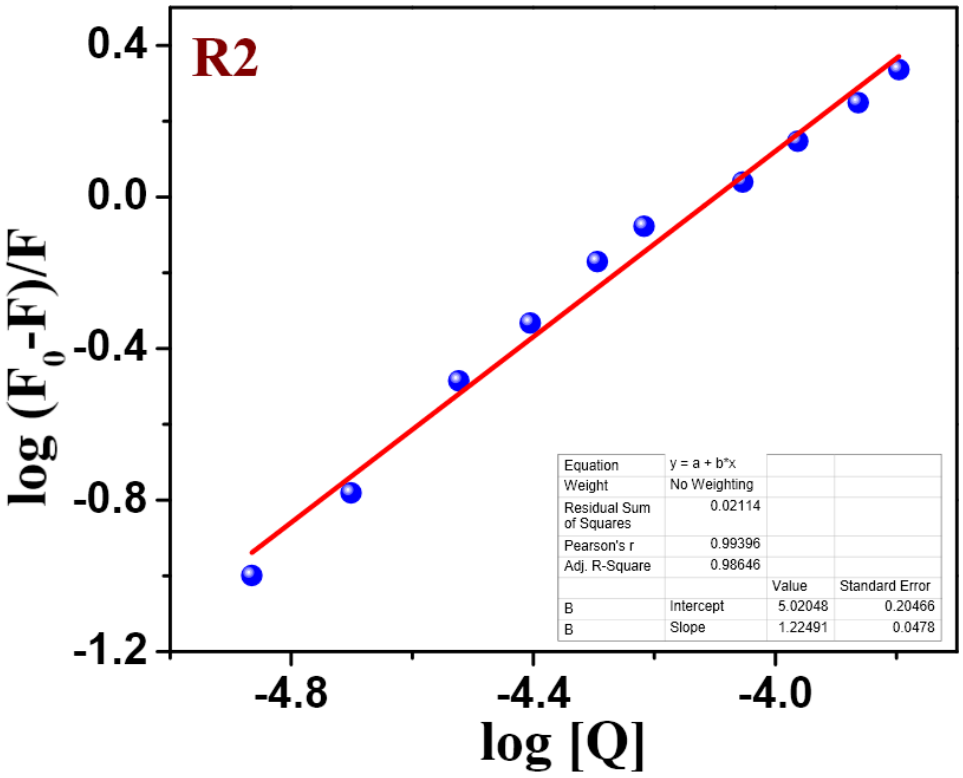
R2
0.4
0.0
-0.4
-0.8
-1.2
log (F0-F)/F
-4.8
-4.4
-4.0
log [Q]
Equation y = a + b*x
Weight No Weighting
Residual Sum of Squares 0.02114
Pearson's r 0.99396
Adj. R-Square 0.98646
Value Standard Error
B Intercept 5.02048 0.20466
B Slope 1.22491 0.0478

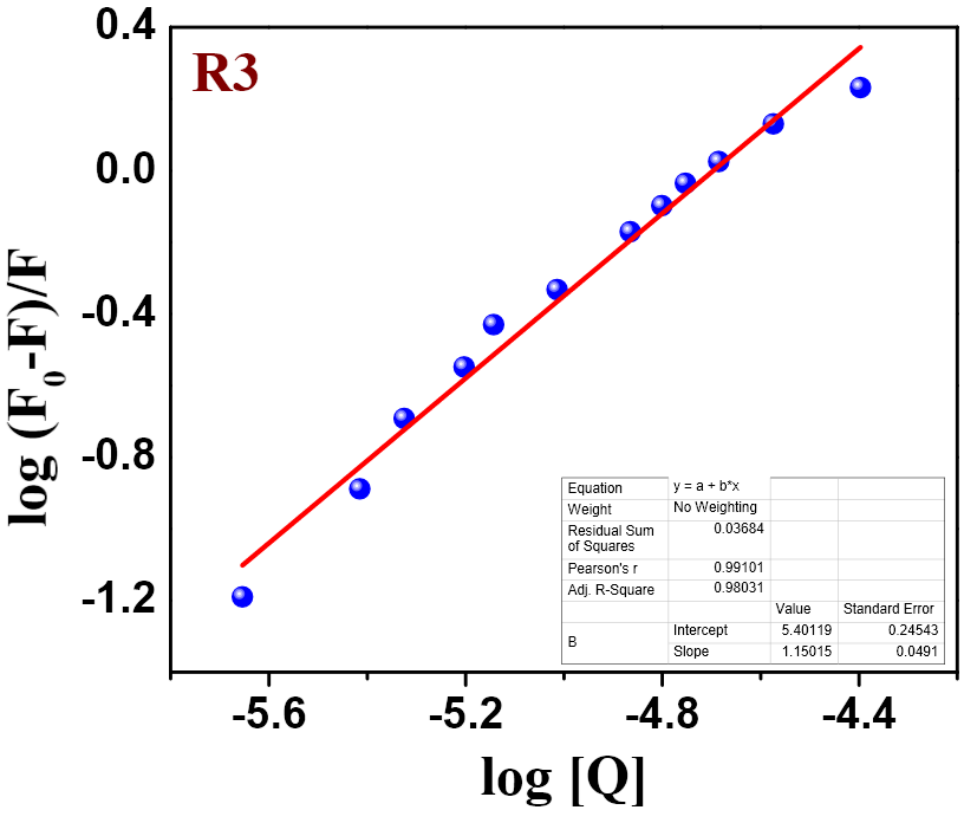
R3
0.4
0.0
-0.4
-0.8
-1.2
log (F0-F)/F
-5.6
-5.2
-4.8
-4.4
log [Q]
Equation y = a + b*x
Weight No Weighting
Residual Sum of Squares 0.03684
Pearson's r 0.99101
Adj. R-Square 0.98031
Value Standard Error
B Intercept 5.40119 0.24543
Slope 1.15015 0.0491

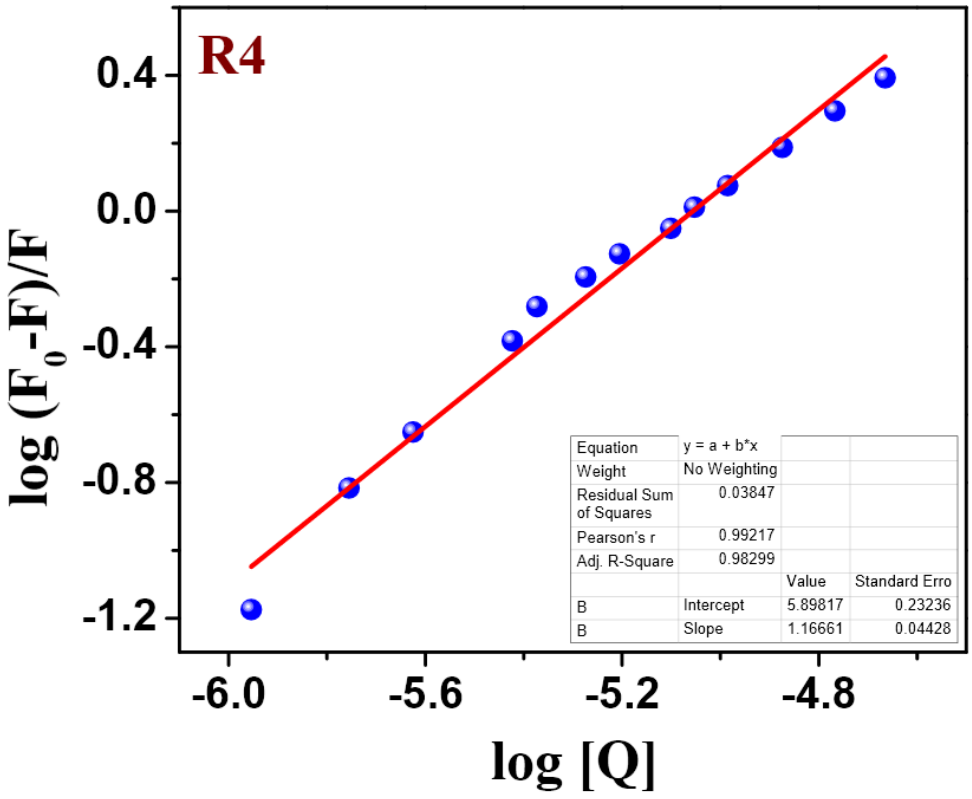
R4
0.4
0.0
-0.4
-0.8
-1.2
log (F0-F)/F
-6.0
-5.6
-5.2
-4.8
log [Q]
Equation y = a + b*x
Weight No Weighting
Residual Sum of Squares 0.03847
Pearson's r 0.99217
Adj. R-Square 0.98299
Value Standard Erro
B Intercept 5.89817 0.23236
B Slope 1.16661 0.04428

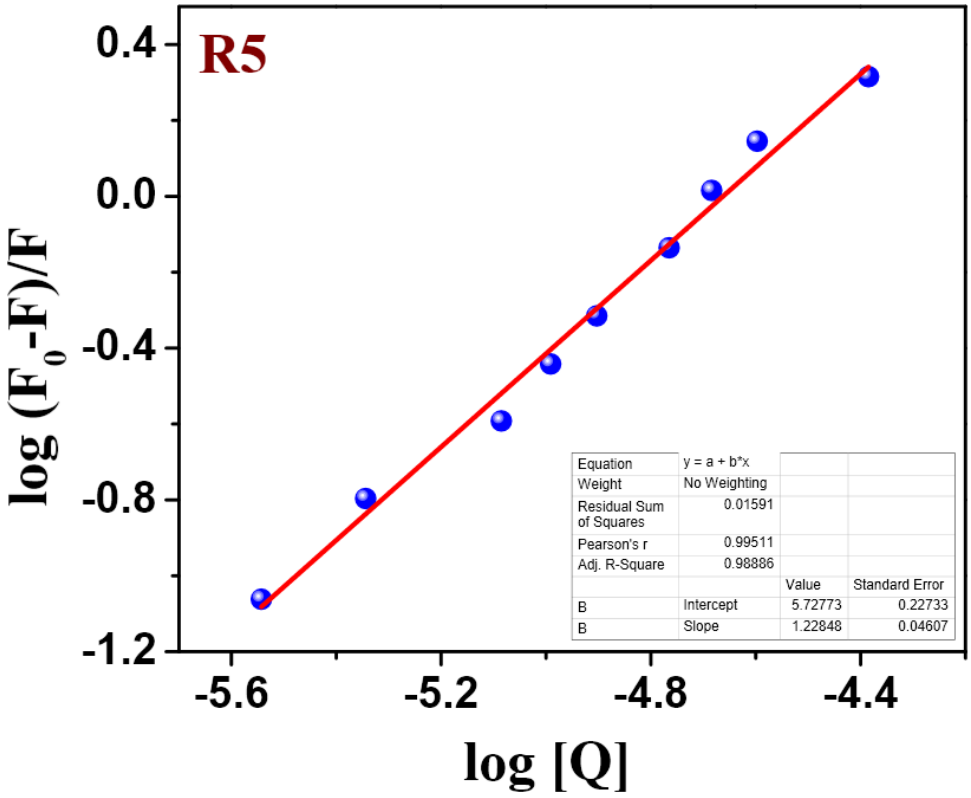
R5
0.4
0.0
-0.4
-0.8
-1.2
log (F0-F)/F
-5.6
-5.2
-4.8
-4.4
log [Q]
Equation y = a + b*x
Weight No Weighting
Residual Sum of Squares 0.01591
Pearson's r 0.99511
Adj. R-Square 0.98886
Value Standard Error
B Intercept 5.72773 0.22733
B Slope 1.22848 0.04607

Fig. S4. Stern-volmer plot of Receptors (**R1-R5**) with F^- ions.

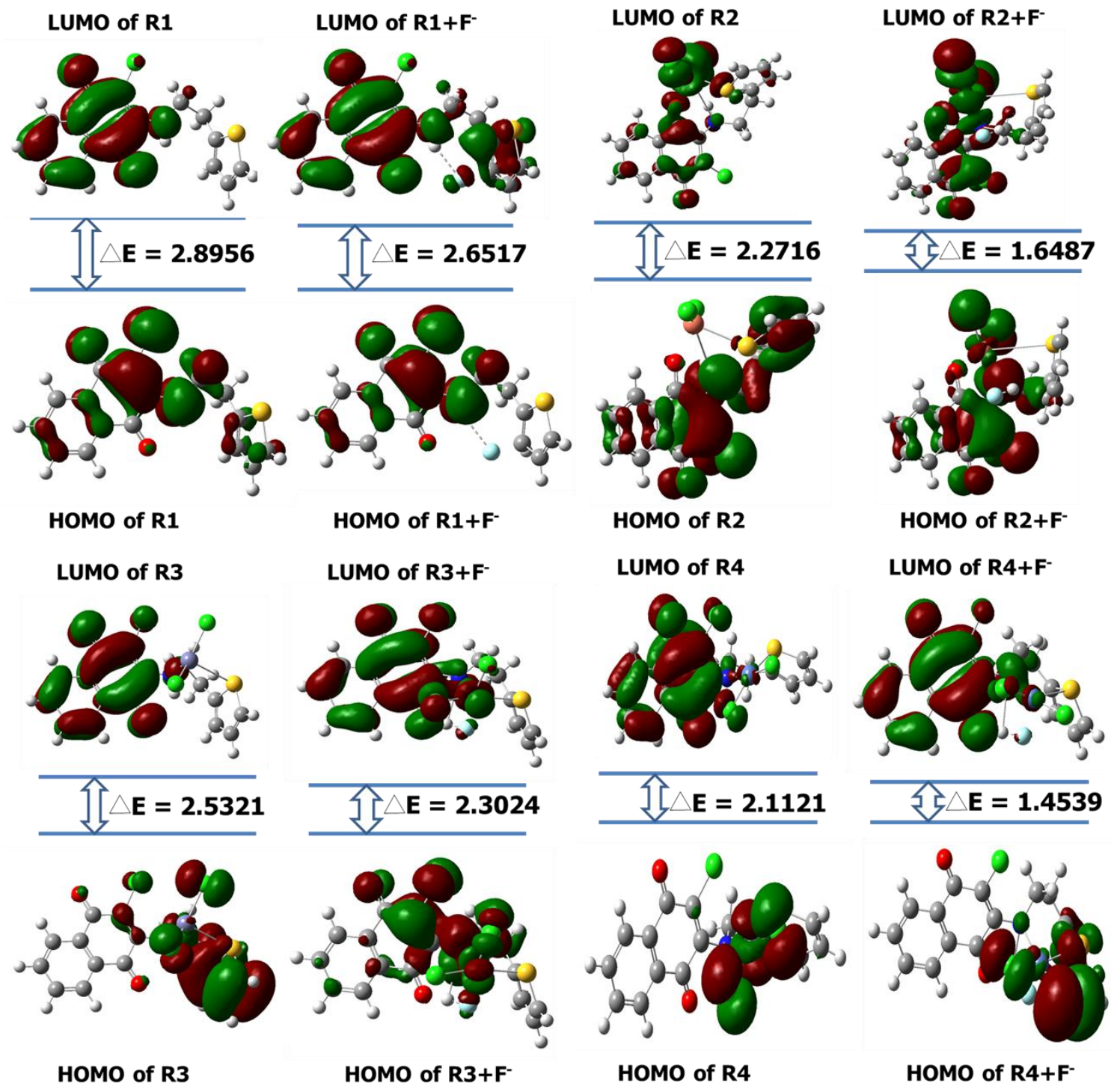
LUMO of R1
LUMO of R1+F-
LUMO of R2
LUMO of R2+F-
△E = 2.8956
△E = 2.6517
△E = 2.2716
△E = 1.6487
HOMO of R1
HOMO of R1+F-
HOMO of R2
HOMO of R2+F-
LUMO of R3
LUMO of R3+F-
LUMO of R4
LUMO of R4+F-
△E = 2.5321
△E = 2.3024
△E = 2.1121
△E = 1.4539
HOMO of R3
HOMO of R3+F-
HOMO of R4
HOMO of R4+F-

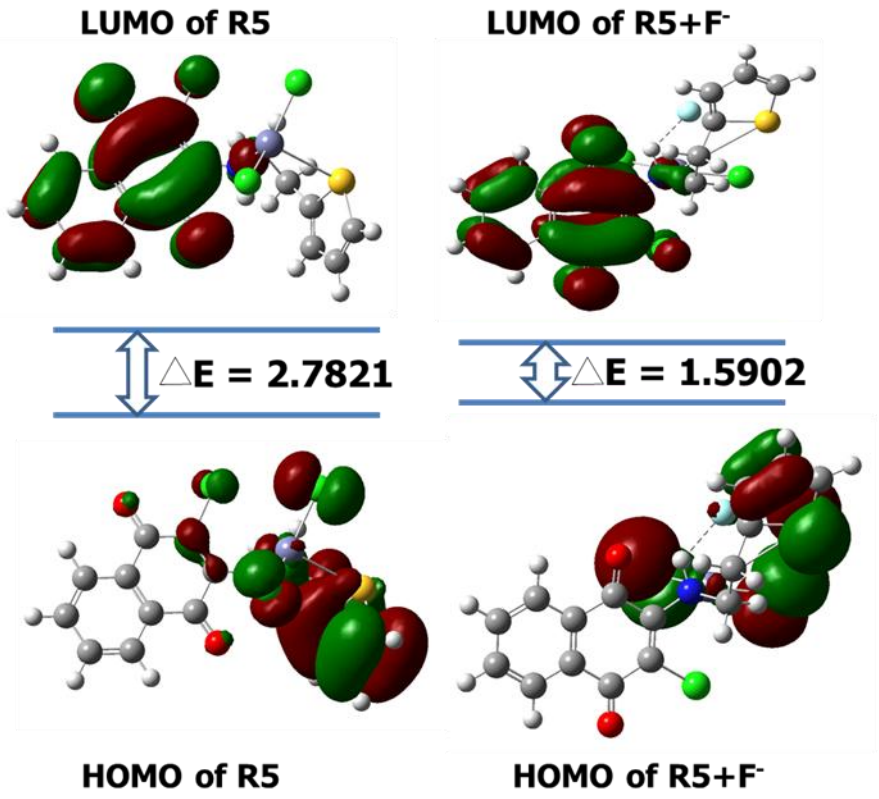

Fig. S5. Electron density distribution of HOMO and LUMO of the free Receptors and their F^- ion complexes.

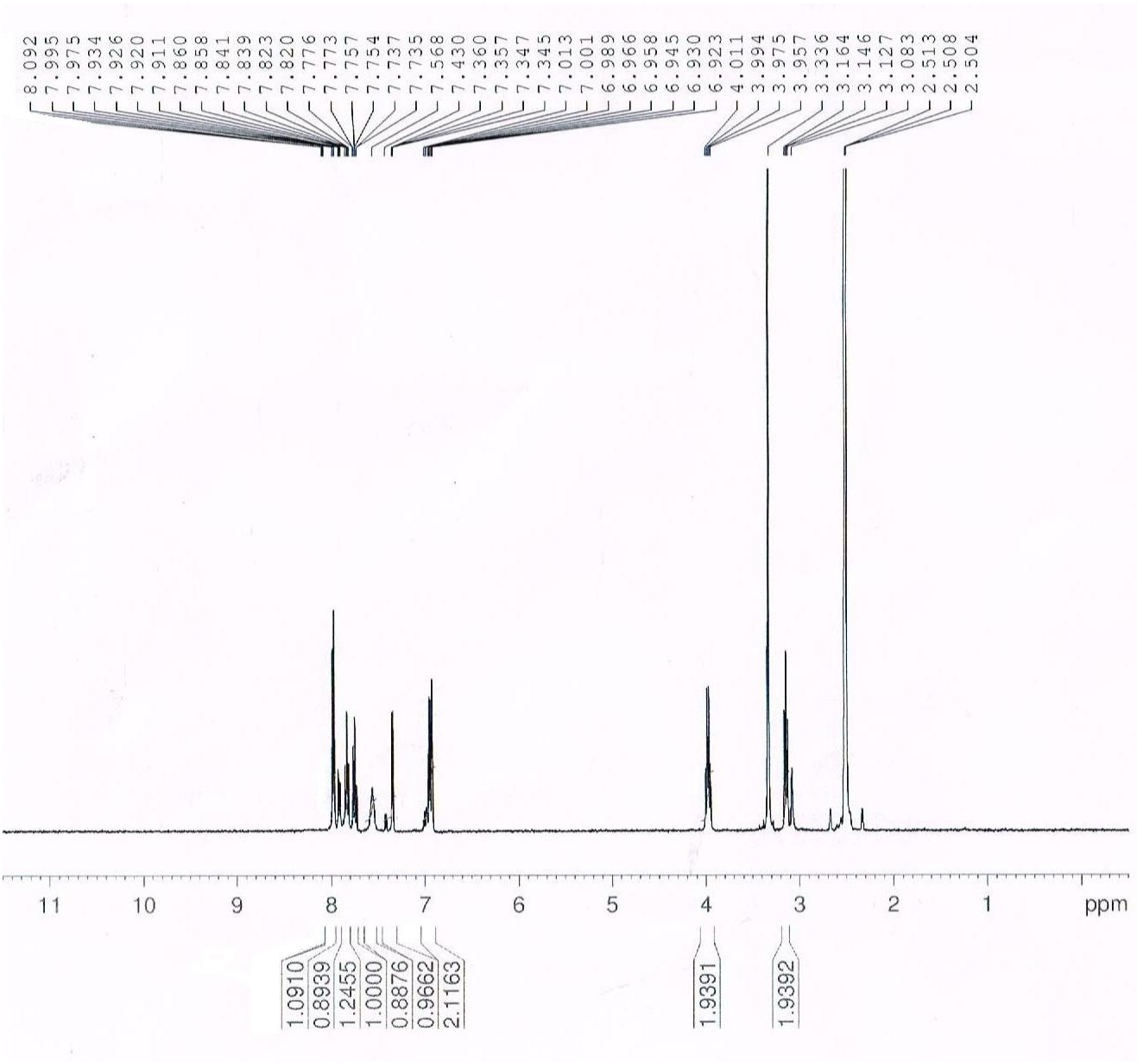

Fig. S6.[1]H NMR spectrum of **R1**

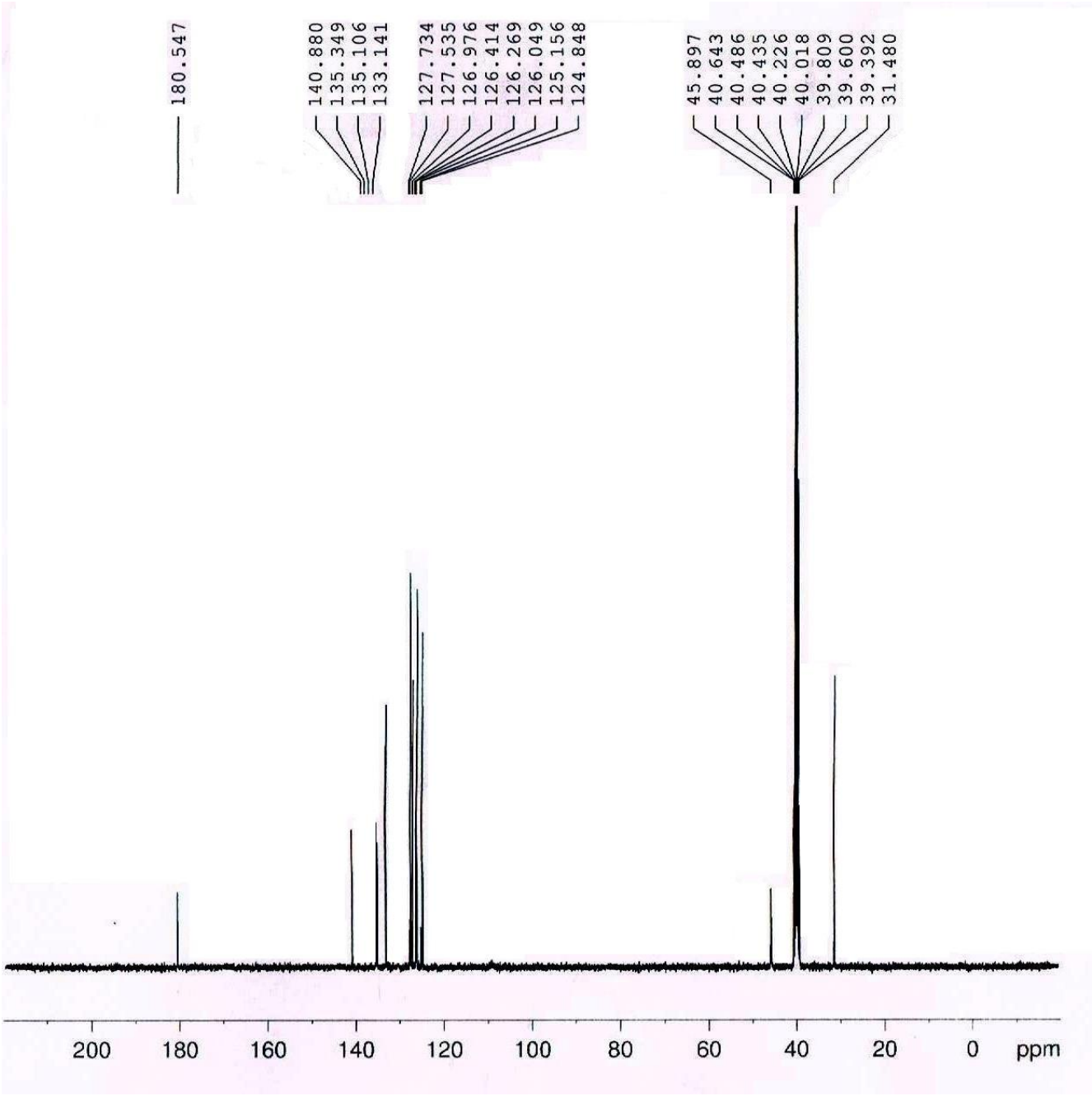

Fig. S7. ^{13}C NMR spectrum of **R1**

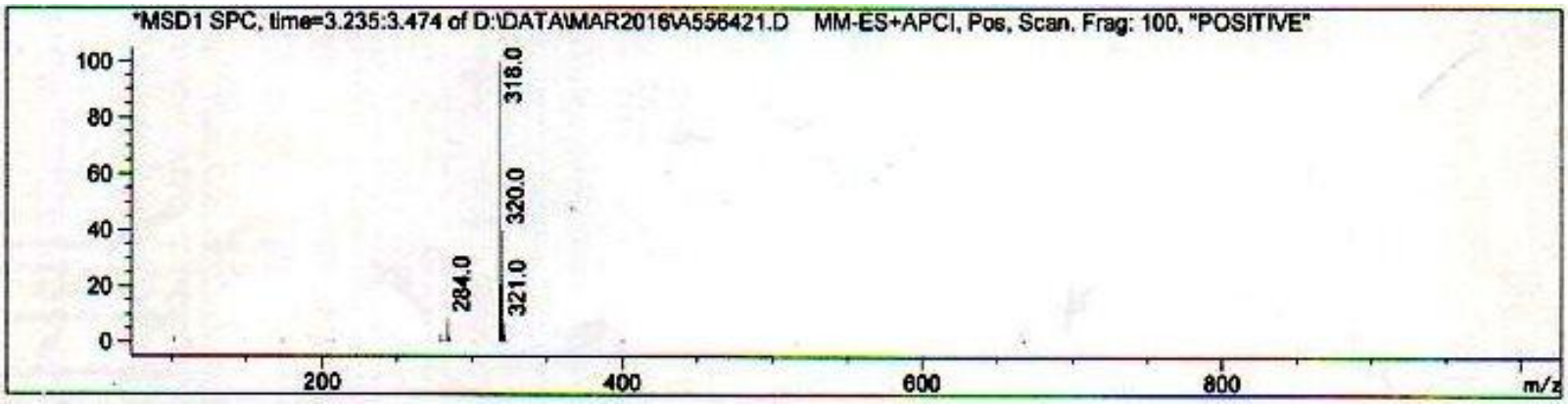

Fig. S8. LCMS spectrum of **R1**

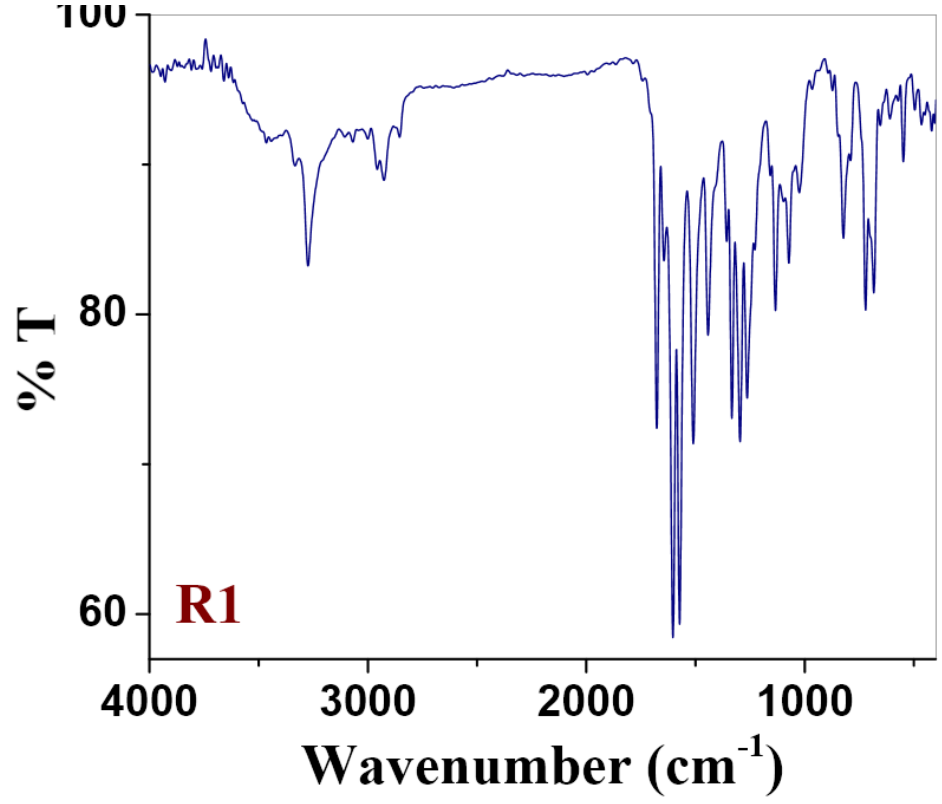
100
80
60
% T
R1
4000
3000
2000
1000
Wavenumber (cm-1)

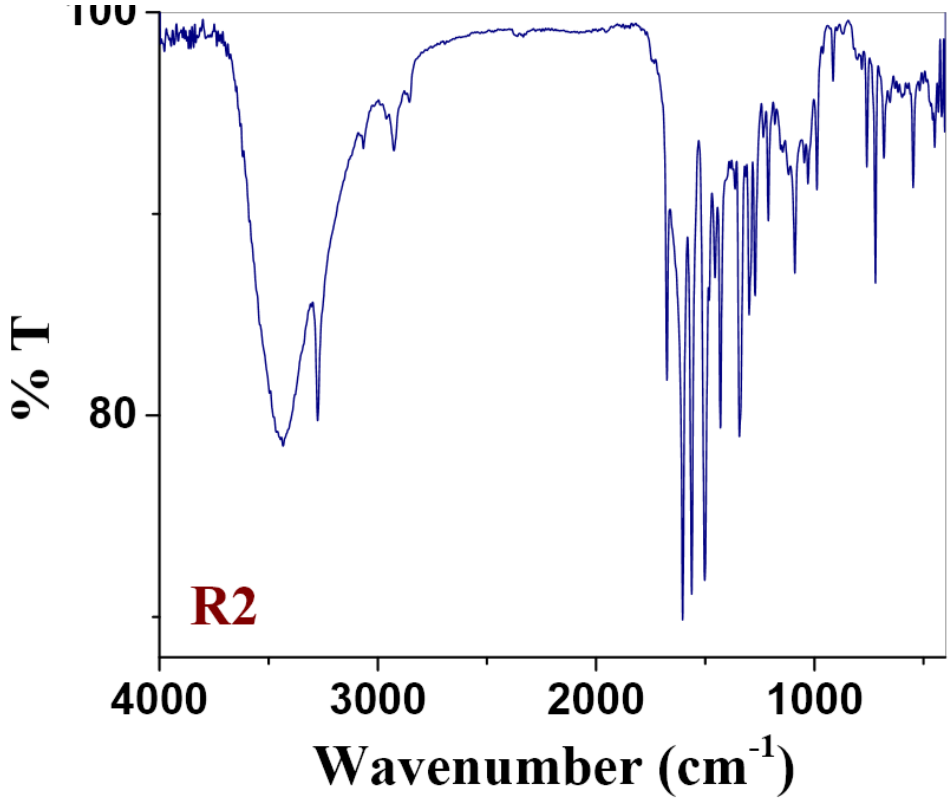
100
80
% T
R2
4000
3000
2000
1000
Wavenumber (cm-1)

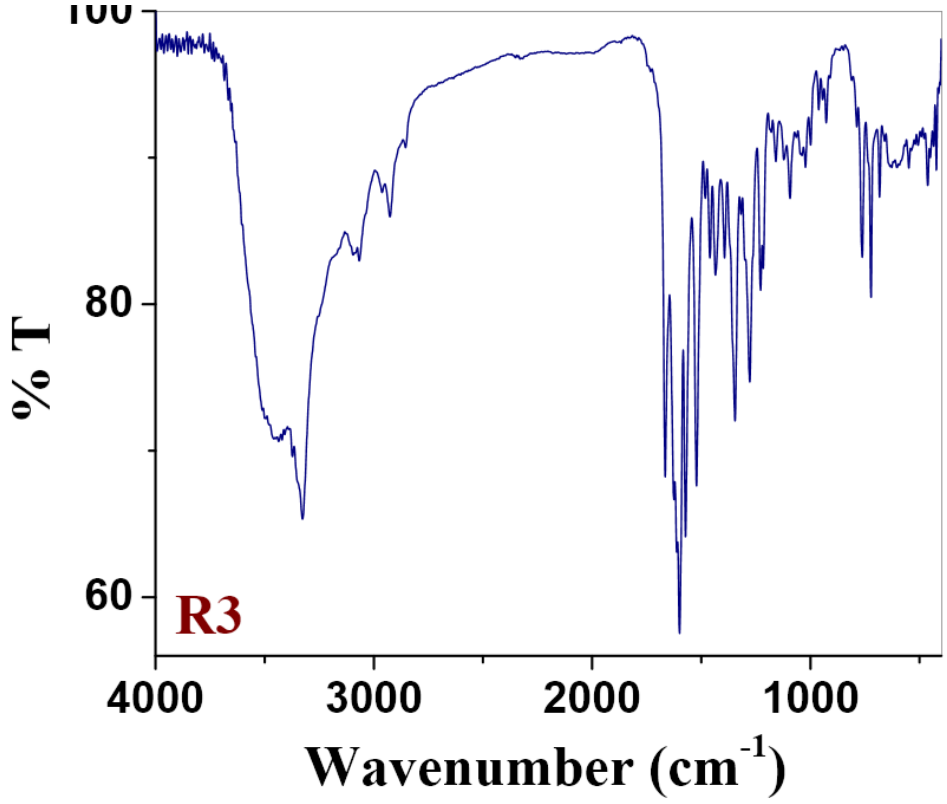
100
80
60
% T
R3
4000
3000
2000
1000
Wavenumber (cm-1)

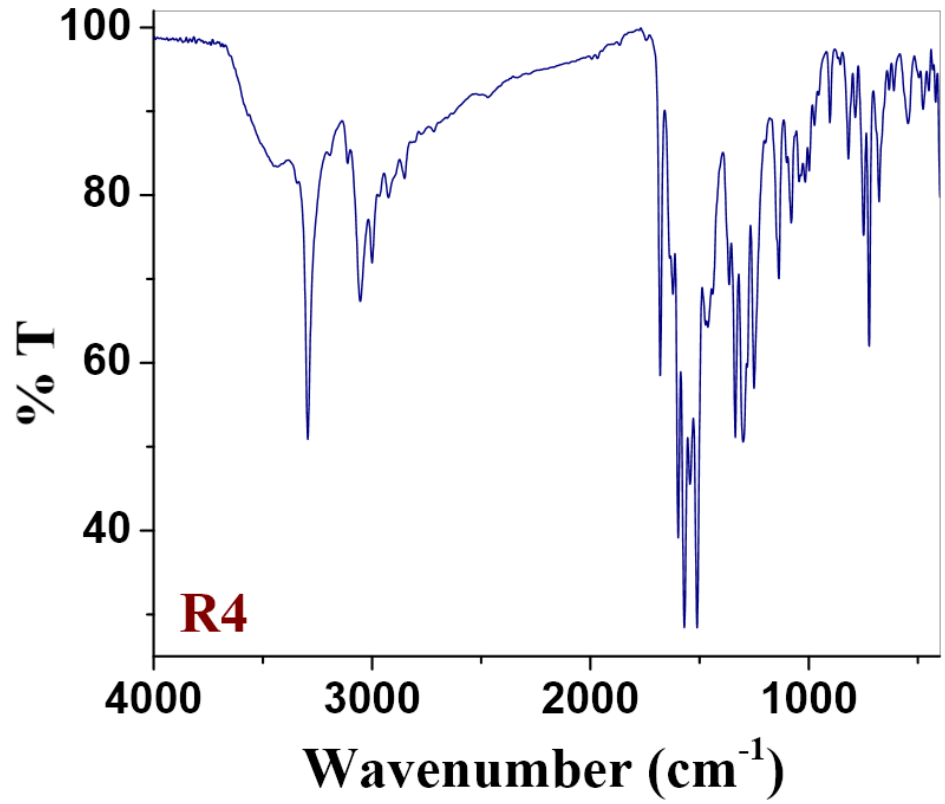
100
80
60
40
% T
R4
4000
3000
2000
1000
Wavenumber (cm-1)

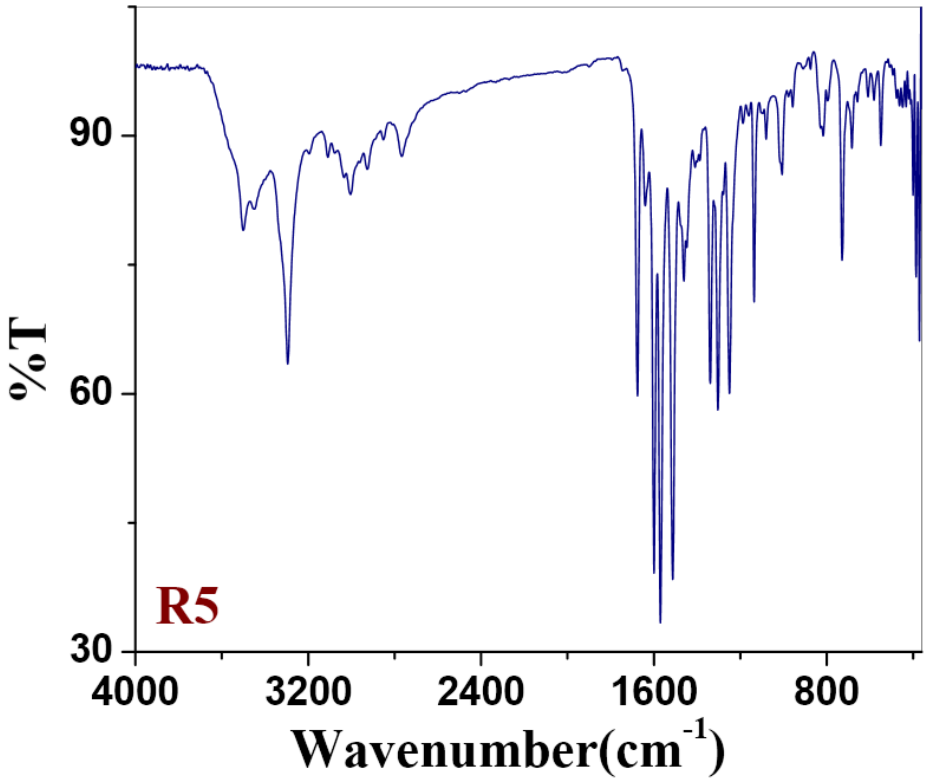

Fig. S9. IR spectra of receptors **R1**-**R5**.

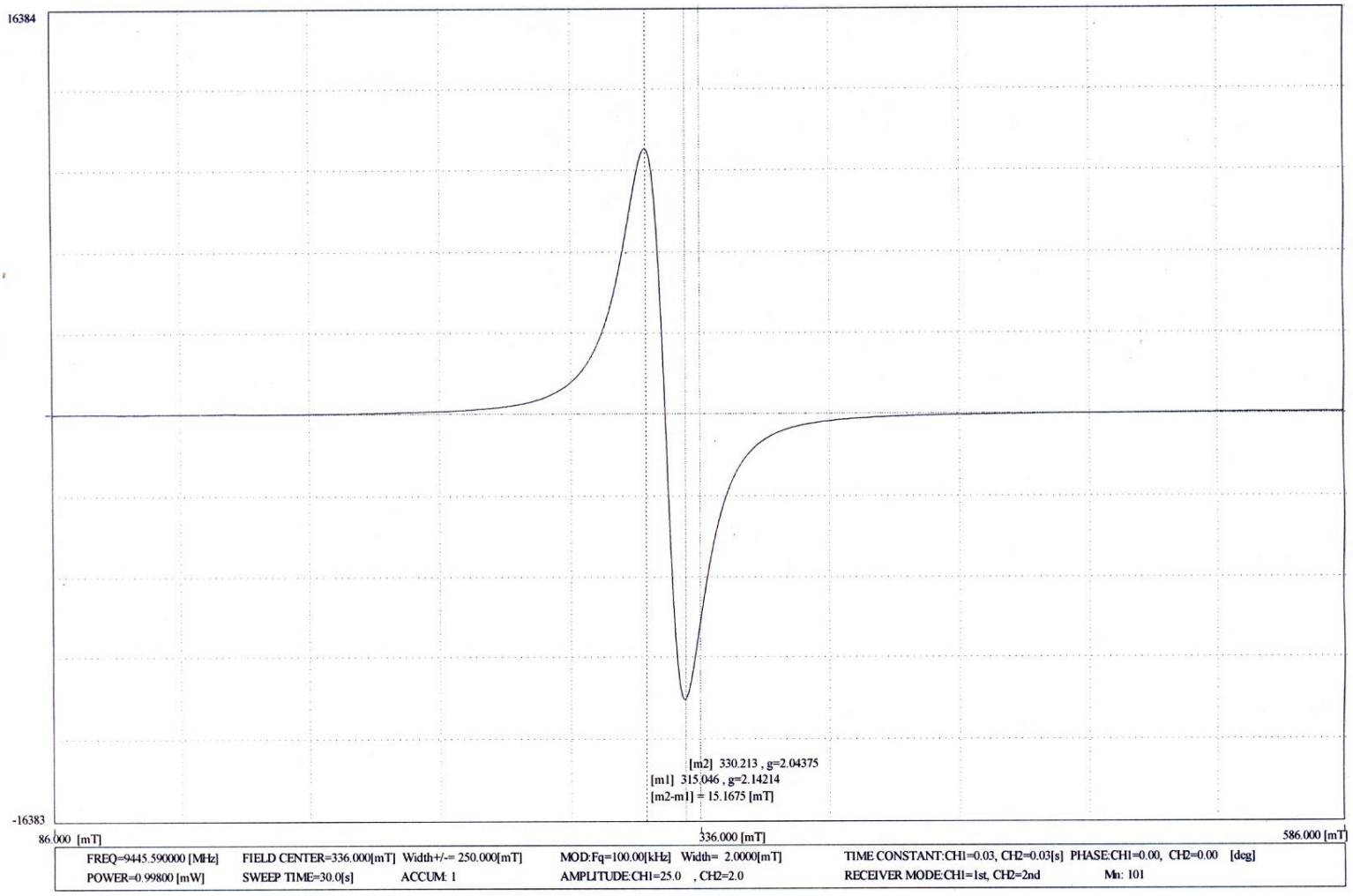

Fig. S10. EPR Spectrum of the Cu(II) Complex.

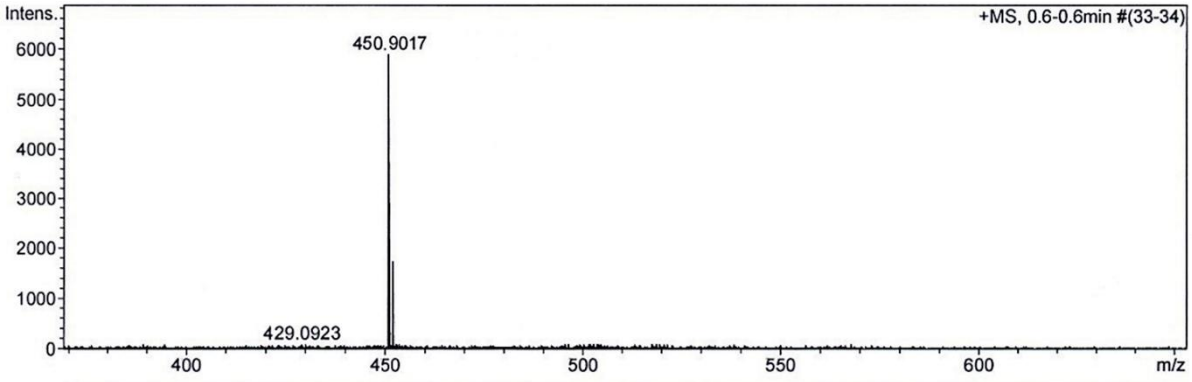
Intens.
+MS, 0.6-0.6min #(33-34)
450.9017
429.0923
m/z

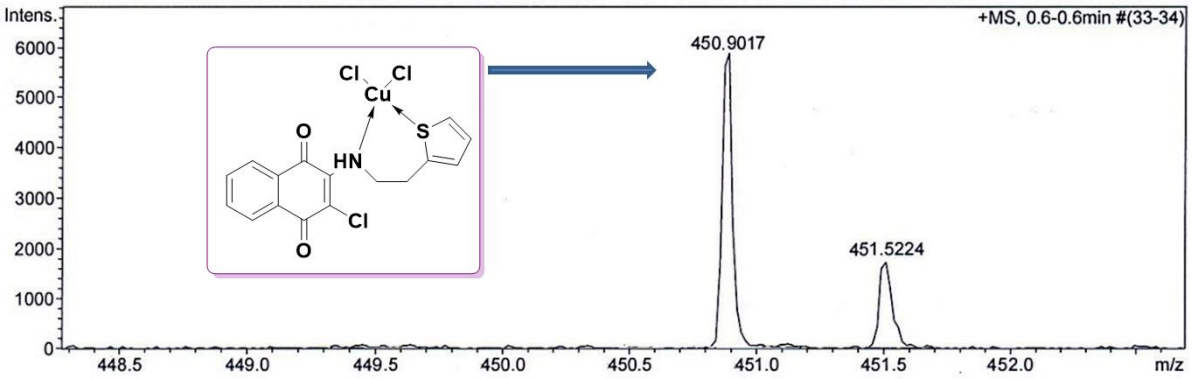
Intens.
+MS, 0.6-0.6min #(33-34)
Cl
Cl
Cu
S
O
HN
Cl
O
450.9017
451.5224
m/z

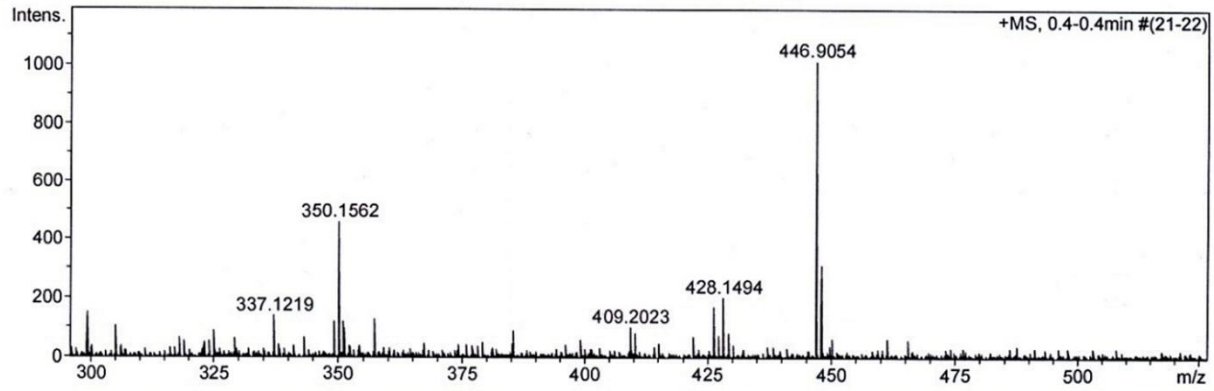
Intens.
+MS, 0.4-0.4min #(21-22)
446.9054
350.1562
337.1219
409.2023
428.1494
m/z

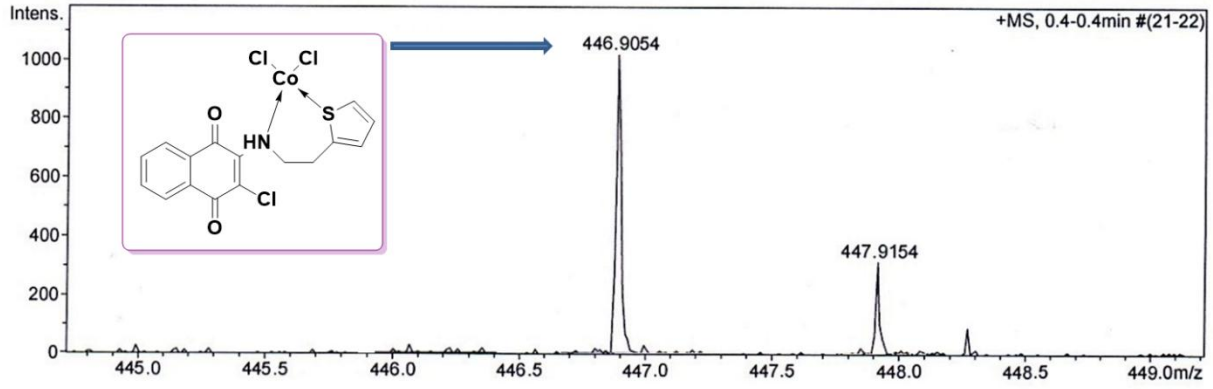
Intens.
+MS, 0.4-0.4min #(21-22)
Cl
Cl
Co
S
O
HN
Cl
O
446.9054
447.9154
m/z

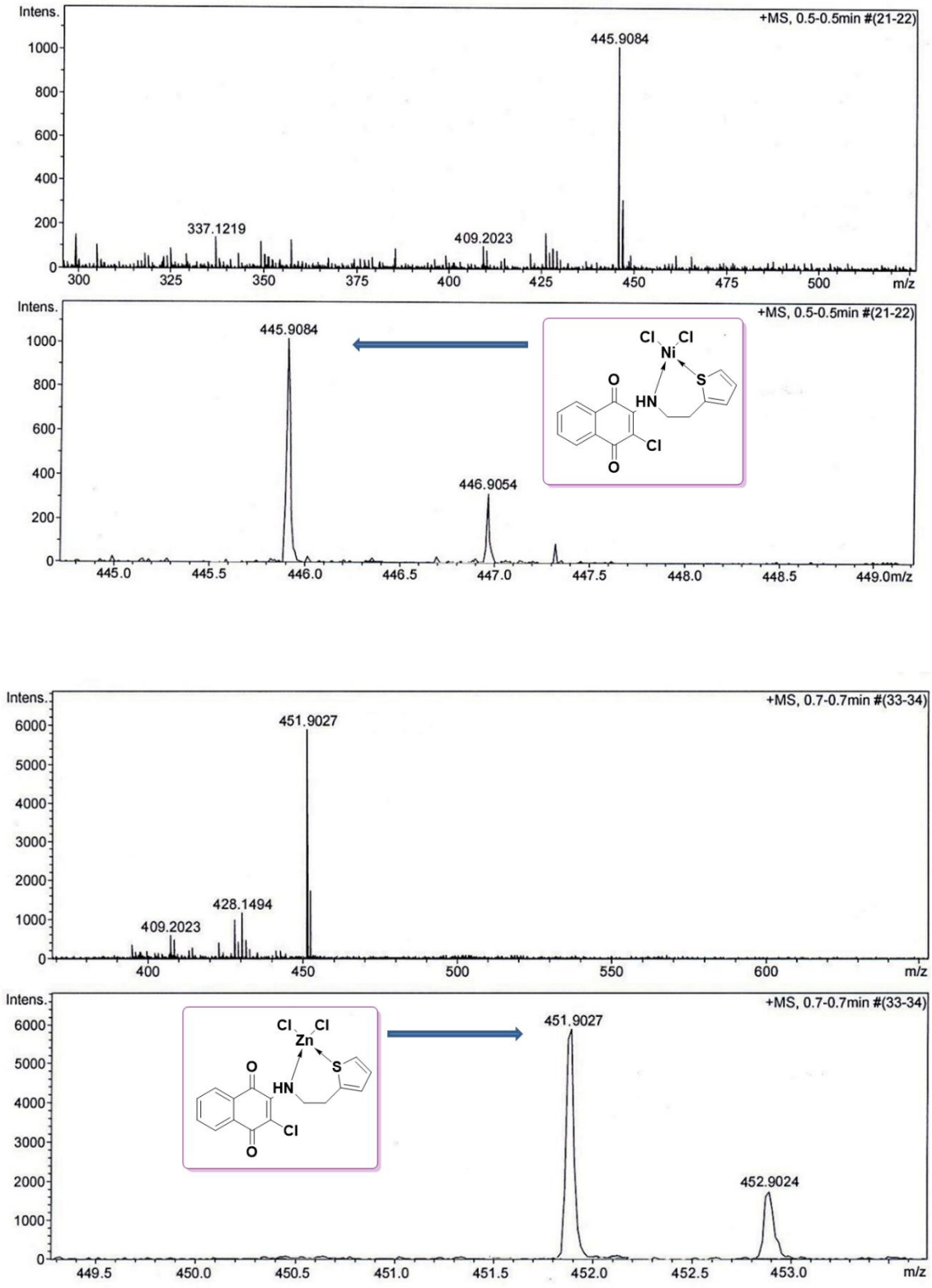

Fig. S11. HRMS spectra of receptors **R2-R5**.

Table S1. Crystal data and structure refinement of **R1**.

Empirical formula	$C_{16}H_{12}ClNO_2S$
Formula weight	317.78
Temperature	293(2) K
Wavelength	0.71073 A
Crystal system, space group	Monoclinic, C c
Unit cell dimensions	a = 23.6442(12) Å alpha = 90 deg.
	b = 4.2788(2) Å beta = 90.614(4) deg.
	c = 14.2732(7) Å gamma = 90 deg.
Volume	1443.92(12) A^3
Z, Calculated density	4, 1.462 Mg/m^3
Absorption coefficient	0.412 mm^-1
Theta range for data collection	4.454 to 29.422 deg.
Limiting indices	-30<=h<=31, -5<=k<=5, -18<=l<=19
Reflections collected / unique	10345 / 3397 [R(int) = 0.0481]
Completeness to theta = 26.00	100.0 %
Max. and min. transmission	0.905 and 1.255
Refinement method	Full-matrix least-squares on F^2
Data / restraints / parameters	3397/ 2 / 226
Goodness-of-fit on F^2	1.042
Final R indices [I>2sigma(I)]	R1 = 0.0453
R indices (all data)	R1 = 0.0586, wR2 = 0.1254
Largest diff. peak and hole	0.283 and -0.226 e.A^-3

Table S2. Bond lengths [A] and angles [deg] for **R1**.

Cl1 C9	1.736(4)
S1 C16	1.697(7)
S1 C13	1.703(4)
O2 C7	1.215(5)
O1 C10	1.228(5)
N1 C8	1.337(5)
N1 C11	1.452(5)
N1 H1N	0.82(5)
C8 C9	1.372(6)
C8 C7	1.522(5)
C9 C10	1.442(5)
C14 C15	1.415(7)
C14 C13	1.432(6)
C14 H14	0.93
C10 C5	1.487(6)
C7 C6	1.462(5)
C5 C6	1.390(6)
C5 C4	1.394(6)
C11 C12	1.527(5)
C11 H11A	0.83(5)
C11 H11B	1.00(4)
C13 C12	1.503(6)
C6 C1	1.402(6)
C12 H12B	1.03(5)
C12 H12A	1.25(6)
C1 C2	1.380(6)
C1 H1	0.90(6)
C4 C3	1.377(7)
C4 H4	0.89(7)
C2 C3	1.394(7)
C2 H2	0.94(6)
C3 H3	0.90(5)
C15 C16	1.329(10)
C15 H15	0.93
C16 H16	0.93
C16 S1 C13	92.4(3)
C8 N1 C11	131.3(3)
C8 N1 H1N	109(4)
C11 N1 H1N	119(4)
N1 C8 C9	130.7(4)
N1 C8 C7	111.0(3)
C9 C8 C7	118.3(3)
C8 C9 C10	123.4(4)
C8 C9 Cl1	122.7(3)
C10 C9 Cl1	113.8(3)
C15 C14 C13	108.9(4)
C15 C14 H14	125.5
C13 C14 H14	125.5
O1 C10 C9	121.5(4)
O1 C10 C5	120.3(4)
C9 C10 C5	118.1(3)
O2 C7 C6	122.7(3)
O2 C7 C8	118.4(3)
C6 C7 C8	118.9(3)
C6 C5 C4	119.9(4)
C6 C5 C10	120.8(3)
C4 C5 C10	119.3(4)
N1 C11 C12	112.9(3)
N1 C11 H11A	110(3)
C12 C11 H11A	106(3)
N1 C11 H11B	110(2)
C12 C11 H11B	112(2)
H11A C11 H11B	106(4)
C14 C13 C12	126.7(4)
C14 C13 S1	111.2(3)
C12 C13 S1	122.1(3)
C5 C6 C1	119.9(4)
C5 C6 C7	120.4(3)
C1 C6 C7	119.7(4)
C13 C12 C11	111.8(3)
C13 C12 H12B	111(3)
C11 C12 H12B	116(2)
C13 C12 H12A	101(3)
C11 C12 H12A	115(3)
H12B C12 H12A	102(3)
C2 C1 C6	119.7(4)
C2 C1 H1	116(4)
C6 C1 H1	123(4)
C3 C4 C5	120.0(5)
C3 C4 H4	122(4)
C5 C4 H4	118(4)
C1 C2 C3	120.2(4)
C1 C2 H2	119(3)
C3 C2 H2	121(3)

C4 C3 C2	120.3(4)
C4 C3 H3	122(3)
C2 C3 H3	117(3)
C16 C15 C14	115.4(5)
C16 C15 H15	122.3
C14 C15 H15	122.3
C15 C16 S1	112.1(4)
C15 C16 H16	124
S1 C16 H16	124

Table. S3. Theoretical data of the receptor and its Complexes.

Receptors	HOMO (eV)	LUMO (eV)	ΔE (eV)
R1	-6.0736	-3.1780	2.8956
R1 + F^-	-5.6546	-2.9723	2.6517
R2	-6.7158	-4.1976	2.2716
R2 + F^-	-6.7150	-5.0662	1.6487
R3	-6.2435	-3.6687	2.5748
R3 + F^-	-6.1335	-3.8311	2.3024
R4	-6.0409	-3.9288	2.1121
R4 + F^-	-6.4611	-5.0072	1.4539
R5	-6.8431	-4.0610	2.7821
R5 + F^-	-5.7805	-4.1898	1.5902

Table. S4. Analytical and physical data of Receptores.

Receptor	Elemental analysis, found (calcd) %			Molar conductance (Ohm^{-1} cm^2 $mole^{-1}$)	μ_{eff} (B.M)
	C	H	N		
R1	60.56 (60.47)	3.85 (3.81)	4.43 (4.41)	---	---
R2	42.57 (42.49)	2.70 (2.67)	3.12 (3.10)	19	1.74
R3	42.97 (42.93)	2.74 (2.70)	3.15 (3.13)	21	2.53
R4	42.99 (42.96)	2.76 (2.70)	3.16 (3.13)	16	Dia
R5	42.41 (42.32)	2.69 (2.66)	3.11 (3.08)	15	Dia

Table. S5. FT-IR spectral data of the R1 and its complexes (cm^{-1})

Compound / Complex	N-H	C=O	C-S	C-S-C	M-N	M-Cl
R1	3274	1603, 1677	721	654	---	---
Cu(II)	3292	1605, 1679	711	668	462	385
Co(II)	3323	1600, 1672	705	670	455	382
Ni(II)	3297	1604, 1679	708	667	458	384
Zn(II)	3299	1602, 1677	707	671	453	383

Characterization of metal complexes

New Cu(II), Co(II), Ni(II) and Zn(II) complexes of the receptor **R1** were synthesized and characterized using analytical and spectral techniques. The complexes were found to be stable in air and soluble in DMF and DMSO. The analytical data of the receptor **R1** and its complexes are summarized in Table S4. The elemental analysis results suggested that the general formula of the complexes is [M(**R1**)Cl_2] {where M= Cu(II), Co(II), Ni(II) and Zn(II)}. The molar conductivity data for 1 mM DMF solutions of the complexes suggested that they are non-electrolyte in nature.[1] The major bands observed in the FT-IR spectra of **R1** and its metal complexes are listed in Table S5. The FT-IR spectra of the complexes were compared with that of free **R1** (Fig. S9) in order to ascertain the mode of coordination of **R1** with the metal ions. The FT-IR spectrum of the free **R1** exhibited characteristic absorption bands at 1603 and 1677 cm^{-1} due to C=O stretching. The two bands observed for the ν(C=O) is well supported by the two different lengths of the C=O bond as shown in the crystal structure of **R1**. In the complexes, these bands remained almost unchanged suggesting non-involvement of the carboxyl oxygen in complexation with the metal ions.[2] The band at 3274 cm^{-1} which corresponds to N-H stretching in the FT-IR spectrum of free **R1** was shifted upwards by 18-49 cm^{-1} in all the complexes indicating the coordination of the N-atom to the metal ions.[19] Additional bands in the region 453-462 cm^{-1} and 382-385 cm^{-1} in these complexes have tentatively been assigned to ν(M-N) and ν(M-Cl) modes, respectively.[20] The shift of ν(C-S)+δ(ring) to lower wavenumbers and the shift of ν(C-S-C) to higher wavenumbers in the complexes, when compared to that in free **R1** have suggested the coordination of **R1** through thiophene ring.[3]

The electronic spectrum of **R1** in DMF exhibited a band at 469 nm (log ε = 3.47) characteristic of the ICT transition from N-H group (donor) to quinone moiety (acceptor).[4] In all

the complexes this band has experienced a blue shift of 2-10 nm. This is due to the fact that coordination of the N-atom with the metal ion would remove the electron density on the N-atom and thereby makes the ICT transition relatively difficult which consequently shifts the band hypsochromically. This observation strongly supported the coordination of the N-atom (of N-H group) with the metal ions as discussed in the FT-IR spectral studies. The electronic spectrum of [Cu(**R1**)Cl_2] showed a broad band at 608 nm assignable to $^2B_{1g} \rightarrow {}^2A_{lg}$ transition which corresponds to a square planar geometry around the Cu(II) ion. The observed magnetic moment of 1.74 BM further supported the electronic spectral results.[19] The EPR spectrum of the Cu(II) complex is solid state at 298 K exhibited axial signals with two g-values, $g_{\parallel}$= 2.1421 and $g_{\perp}$= 2.0437 (Fig. S10). In square planar complexes the unpaired electron lies in d_{x2-y2} orbital giving $^2B_{1g}$ as the ground state with $g_{\parallel} > g_{\perp}$. In the present case, the observed trend $g_{\parallel} > g_{\perp} > g_e$ (2.0023) confirmed the square planar nature of [Cu(**R1**)Cl_2].[5]

The electronic spectrum of [Co(**R1**)Cl_2] exhibited two bands at 604 and 672 nm assignable to $^4A_{2g} \rightarrow {}^4T_{1g}{}^{(P)}$ and $^4A_{2g} \rightarrow {}^4T_{1g}{}^{(F)}$ transitions, respectively suggesting a square planar geometry for the complex. The observed magnetic moment of 2.53 BM further corroborated the electronic spectral finding.[20,6] The diamagnetic nature of [Ni(**R1**)Cl_2] revealed by magnetic moment studies confirmed the square planar environment around the Ni(II) ion.[7] The Zn(II) complex was found to be diamagnetic as expected for d^{10} configuration. The shifts observed in the FT-IR bands when compared to that of free **R1** indicated the coordination of the S- and N-atoms from the **R1** and two chloride ions from the metal salt making up a four coordination sphere for the tetrahedral coordinated geometry.[8] The HRMS spectra of the complexes were recorded and are depicted in figure. S11, which confirmed the proposed formulae.

1 S. Madhupriya and K. P. Elango, *Synth. React. Inorg. Met-Org and Nano-Met. Chem*., 2014, **44**, 1104-1119.

2 C. Parthiban and K. P. Elango, *Sens. Actuators B*, 2016, **237**, 284-290.

3 F. Hamurcu, A. B. Gunduzalp, S. Cete and B. Erk, *Transition Met. Chem*., 2008, **33**, 137-141.

4 A. Satheshkumar, K. Ganesh and K. P. Elango, *New J. Chem*., 2014, **38**, 993-1003.

5 V. P. Singh, S. Singh, D. P. Singh, K. Tiwari and M. Mishra, *J. Mol. Struct*., 2014, **1058**, 71-78.

6 E. Kent Barefield, D. H. Busch and S. M. Nelson, *Q. Rev. Chem. Soc*., 1968, **22**, 457-498.

7 J. P. Barbier, A. E. Biyyadh, C. Kappenstein, N. D. Mabiala and R. P. Hugel, *Inorg. Chem*., 1985, **24**, 3615-3620.

8 P. Tyagi, S. Chandra and B. S. Saraswat, *Spectrochim. Acta A*, 2015, **134**, 200-209.